Journal Pre-proof

Kinetics of pressurized oxy-combustion of coal chars

Piotr Babiński, Grzegorz Łabojko, Michalina Kotyczka-Morańska, Marek Ściążko

PII: S0040-6031(19)30542-8

DOI: https://doi.org/10.1016/j.tca.2019.178417

Reference: TCA 178417

To appear in: *Thermochimica Acta*

Received Date: 17 June 2019

Revised Date: 3 September 2019

Accepted Date: 22 September 2019

Please cite this article as: Babiński P, Łabojko G, Kotyczka-Morańska M, Ściążko M, Kinetics of pressurized oxy-combustion of coal chars, *Thermochimica Acta* (2019), doi: https://doi.org/10.1016/j.tca.2019.178417

Kinetics of pressurized oxy-combustion of coal chars

Piotr Babiński, Grzegorz Łabojko*, Michalina Kotyczka-Morańska, Marek Ściążko

Institute for Chemical Processing of Coal
1 Zamkowa, 41-803 Zabrze, Poland

* Corresponding author. Tel.: +48 32 271-00-41, ext. 537; fax: +48 32 271-08-09
E-mail address: glabojko@ichpw.pl (Grzegorz Łabojko)

Highlights

- Use of increased pressure influence positively the kinetics of coal oxycombustion reaction
- Reaction rate of oxycombustion is proportional to oxygen concentration raised to the power of reaction
- Selection of the appropriate reaction model must be based on the correlation of differential not integral data
- Random pore model (RPM) is an appropriate model describing the rate of oxycombustion reaction of coal char

Abstract

A kinetic study of oxy-combustion of chars received from two Polish coals, namely lignite and hard subbituminous was conducted. The kinetics of char oxy-combustion was examined in the TA Instruments TG-HP150s pressurized thermogravimetric analyzer at 0.1, 0.5 and 1 MPa of absolute pressure. The experiments were carried out at isothermal conditions and at wide range of temperature (773 – 1273 K). Mixture of gas containing 20% and 30% of O_2 in CO_2 was used as an oxidant. Additionally at temperature 873 K the experiments were performed using 5%, 10% and 40% of O_2 in CO_2. A kinetic model of pressurized oxy-combustion of coal char was presented. Kinetic parameters such as activation energy, pre-exponential factor and reaction order in respect of oxygen concentration were computed. Influence of temperature, pressure and O_2 concentration were discussed. The results show a significant shift of the oxycombustion reaction from kinetically controlled regime to diffusion – controlled regime with increasing temperature and pressure. The method of selecting the proper reaction model was presented based on the integral and differential approach of experimental data analysis.

Keywords Diffusion effects, Kinetics, Oxy-combustion, Char combustion

* Corresponding author. Tel.: +48 32 271-00-41, ext. 537; fax: +48 32 271-08-09
E-mail address: glabojko@ichpw.pl (Grzegorz Łabojko)

List of symbols

HPTGA – high pressure thermogravimetric analyzer

A	surface / m^2
A_0	pre-exponential factor / s^{-1}
AC	ash content / wt %
C	concentration of gas / mol m^{-3}
d	diameter / m
D	diffusion coefficient / m^2 s^{-1}
E_a	activation energy / kJ mol^{-1}
h	height / m
k_D	mass transfer coefficient / m s^{-1}
l	length / m
LHV	lower heating value / J g^{-1}
m	mass / mg
M	moisture content / wt %
N	molar flow rate of gas / mol s^{-1}
P	pressure
r	reaction / diffusion rate / mol s^{-1}
R	universal gas constant / kJ mol^{-1} K^{-1}
R_p	pore radius / m
Re	Reynolds number / -
S	specific surface area / m^2 g^{-1}
Sh	Sherwood number / -
Sc	Schmidt number / -
T	temperature / K
t	time / s
u	velocity of gas / m s^{-1}
V	volatile matter content / wt %
X	conversion degree of solid / -
y	molar fraction / -
β	heating rate / K min^{-1}
μ	viscosity / Pa s
ρ	density / kg m^{-3}
τ_p	tortuosity of the pores / -
ε_0	porosity of the particle / -

Subscripts

ash	relates to mineral matter
b	refers to bed
BET	Brauner-Emmet-Teller
CO_2	related to carbon dioxide
con	refers to convection
D	refers to diffusion / mass transport
D-A	Dubinin-Astachow
eff	effective
ext	refers to external
g	refers to gas
int	refers to internal
K	refers to Knudsen diffusion
N	refers to crucible
me	refers to mesopores
mi	refers to micropores
O2	related to oxygen
obs	observed
R	refers to reaction
t	total
0	refers to initial state

Superscripts

ar	as-received basis
ad	air-dried basis
d	dry basis
daf	dry and ash-free basis

Introduction

Recently, a great attention has been focused on carbon dioxide emissions from a power sector due to the significant impact of greenhouse effect. To reduce the emissions of greenhouse gases from fossil fuel-fired power generation, oxy-combustion of coal seems to be a promising future technology while retrofitting of existing boilers to enable O_2-enriched atmosphere for combustion [1,2].

In the process of oxy-combustion of fossil fuels, an oxygen (above 95 %) and a stream of recycled CO_2, from the flue gas to control the combustion temperature, are used. The process product is a gas consisting mostly of CO_2 and water vapour. Considerable concentration of CO_2 in the gas enables its direct referral to the sequestration, which is followed by water vapour condensation [3,4].

Research on oxygen-enriched, pressurized coal combustion has been conducted since the nineties of the last century and shows that this technology is attractive way of capture and sequestration of CO_2 despite the significant increase of energy consumption [5]. This technology possess high application potential and raises particular interest of the scientific community and manufacturers of steam boilers. Main factors, which improves boiler efficiency with the increase of gas pressure in combustion chamber are as follows [6-8]:

- Pressurized oxycombustion allows better burnout degree of char, which is a product of first stage of coal thermal decomposition i.e. pyrolysis.
- The coefficient of thermal conductivity in the convection zone of the boiler increases.
- Increased pressure of exhaust gases causes shift of steam dew point towards higher temperature, which allows recuperation of energy from steam condensation.
- Pressurized stream of oxygen is obtained from low-temperature installation of air fractioning which lowers costs of compressing CO_2 from oxycombustion.
- More effective removal of NO_x and SO_x from exhaust gases.
- Oxycombustion runs at pressure between 4.83 – 8.96 MPa and allows to use cooling water from power plant to condensate CO_2 under pressure.

Hong [6] compared oxycombustion at 0,1 MPa with basic case oxycombustion at 1,0 MPa and stated almost 3% netto efficiency increase of energy unit in case of pressurized technology. Performed by these authors simulations and calculations using Thermoflex and Aspen Plus softwares permit to draw conclusion that for pressurized combustion increase of efficiency and lowering investment costs causes decrease of overall costs of energy production, which is mainly due to increased energy recovery from exhaust gases stream (among others by utilization of heat of condensation of water vapour).

The oxy-combustion process comprise several consecutive processes and reactions. When a coal particle is introduced to a combustion chamber of a fluidized bed, it is heated up at a high heating rate (up to 1000 K s^{-1}). This step involves drying and pyrolysis of coal particle, and volatile matter consisted of combustible gases evolving, while char producing. The volatiles burn in homogenous reactions and char reacts with an oxygen (heterogeneous reaction). The reaction of carbon from char with O_2 is the slowest step of the whole process [9-11]. Therefore, the present work focuses on the coal char oxy-combustion, because its reaction rate is crucial for a boiler design. Since the oxy-combustion of coal char is a heterogeneous reaction, therefore it can proceed under three different reaction-controlling regimes: chemical kinetics, mixed internal diffusion–chemical kinetics, and external diffusion regime [12,13]. Oxy-combustion in a fluidized bed boiler occurs at temperature of 1073–

1173 K, where diffusion limitations exist [3,4,14]. The scaling-up of this process requires an extensive computational analysis, which is critical for the proper boilers design. Herein, a kinetic analysis is fundamental for oxy-combustion process modelling, where the kinetic equations are implemented with a modelling software.

On the other hand, thermogravimetric analysis is a commonly used technique to investigate the kinetics of fast heterogeneous reactions such as combustion of solid fuels, oxidation of solid oxygen carriers etc. [9,10,15-23]. It is well known that kinetic parameters should be obtained under chemical reaction controlling regime [9,10,17,18,21-23], which is important for oxy-combustion kinetic study.

Another issue that raises doubts in the literature is the selection of an appropriate model response f(X). The reaction rate dX/dt as a function of extent of conversion of X can take a different course. Changes in a reaction rate depending on the degree of conversion can be presented as a mathematical function, called a reaction model f(X). This function presents the change of rate of the chemical reaction as a function of degree of conversion of solid material. Oxycombustion reaction of char is a heterogeneous one, in which the element C reacts with oxygen and gives CO_2, in gaseous form. During the reaction, the element C of the char is irreversibly consumed, the particle structure of the char is significantly changed, i.e. the internal surface, the particle diameter, the porosity and the apparent density change. All these points should be included in the kinetic equation and presented as a chemical reaction model. There is a wide variety of possible kinetic models describing the course of the chemical reaction and they are deeply analyzed, among others at work [21,24]. The interpretation of the reaction mechanism through the applied model is most often done by the analysing of the fitting of the mathematical model to the rate of the experimentally determined reaction. This approach has been used in this work, however, own validation procedures have been developed, which solves ambiguity in choosing the best model.

Experimental Section

Samples properties

Two char samples obtained from Polish lignite (Turów) and hard subbituminous coal (Janina), which are extensively used for combustion in Polish power plants, were investigated. The chars were prepared using a laboratory stand for the pyrolysis of solid fuels. First, ca. 150 g of coal sample with a size of 1–3.15 mm was placed in a cylindrical batch reactor. Then, the reactor was heated up to 1273 K at a heating rate of 5 K min^{-1} under nitrogen. After that, the reactor was flushed with N_2 to cool down the sample to room temperature. The coal sample and obtained char samples were crushed and sieved to a particle size smaller than 200 μm, and were further analyzed.

The proximate analyses of coal and char samples were determined by a gravimetric method using LECO TGA701. The ultimate analysis that followed sulfur analysis was conducted using CHN TruSpec LECO and LECO SC632 apparatus (Table 1). Porous structure of coal chars was analyzed by nitrogen adsorption at 77 K and CO_2 adsorption at 273 K method by using 3Flex Micromeritics apparatus. (Table 2).

Table 1 Proximate and ultimate analysis of coals

	Lignite	Hard coal
Proximate analysis		
M^{ar} / %	44.2	21.3
M^{a} / %	3.9	12.4
AC / %	7.8	10.4
V^{daf} / %	59.14	39.56
LHV^{a} / MJ kg^{-1}	24.72	22.84
Ultimate analysis		
C^{a} / %	62.30	60.40
H^{a} / %	5.48	3.46
N^{a} / %	0.61	0.94
$S_t{}^{a}$ / %	1.02	1.22
O^{a} / %	18.89	11.18

Table 2 Proximate, ultimate and porous structure analysis of coal chars

	Lignite char	Hard coal char
Proximate analysis		
M^a / %	0.20	0.70
AC^a / %	12.32	15.19
V^{daf} / %	0.00	0.54
Ultimate analysis		
C^a / %	82.50	81.40
H^a / %	0.34	0.35
N^a / %	1.06	0.99
S_t^a / %	0.93	0.65
O^a / %	3.25	1.59
N_2 adsorption at 77 K		
S_{BET} / m^2 g^{-1}	17.3	3.8
V_t / cm^3 g^{-1}	0.0154	0.0448
V_{mi} / cm^3 g^{-1}	0.0091	0.0011
V_{me} / cm^3 g^{-1}	0.0063	0.0438
CO_2 adsorption at 273 K		
S_{D-A} / m^2 g^{-1}	719.3	312.9
V_t / cm^3 g^{-1}	0.2055	0.0322

Raw coal samples were significantly different in terms of metamorphism degree, as indicated by the volatile content, elemental composition, and particularly oxygen content. The pyrolysis of coal led to an increase in element C content to approx. 80 %, and to the reduction of the hydrogen, oxygen, sulfur and nitrogen contents. The analysis results obtained from the coal char indicate that the chemical composition of obtained chars is close to each other, even though they come from coals with different degree of metamorphism. The pyrolysis resulted mainly in a removal of moisture from the coal samples, and in a separation of the volatile components, producing lignite char with zero content of volatiles, and approx. 0.5 % for hard coal char. In other words, the pyrolysis of coal has increased the degree of metamorphism of the parent coal and conformed them chemically to one another. Although, the proximate and ultimate analysis show that the properties of chars are similar, there are some significant differences in their structure. And these have the greatest impact on the char particles reactivity. For example, the char porous structure has a greater impact than its chemical composition. Much smaller specific surface area (determined by BET method) is shown by a sample of hard coal char, and significantly larger surface area discloses lignite char. The surface of the micropores which were determined by adsorption of CO_2 at 273 K, confirmed the greater surface area of the lignite's char micropores.

Thermogravimetric analysis

Oxy-combustion tests were conducted in a pressurized thermogravimeter TG-HP150s from TA Instruments with Rubotherm magnetic suspension balance (HPTGA). Reaction gases were fed with defined composition and specific volume flow to the reaction furnace. The gaseous mixtures with a suitable molar fraction of oxygen y_{O2}

in CO_2 equals to 0.2 and 0.3 were introduced to the TGA. The experiments in the HPTGA were conducted under three different total pressures: 0.1, 0.5 and 1.0 MPa. The char sample weight was m_0 = 10 mg. The influence of oxygen concentration were studied at 500°C for molar fraction of oxygen y_{O2} in CO_2 equals: 0.1, 0.2, 0.3, 0.4, and 0.5 of O_2 in CO_2.

Mathematical modeling

The rate of the chemical reaction for isothermal conditions can be represented by the expression (1) [10]:

$$r = \frac{dX}{dt} = kC_{O2}^{n} f(X) = k' f(X) \quad (1)$$

Where: d*X*/d*t* – rate of the chemical reaction *f(X)* – chemical reaction model for the differential form of the kinetic equation, *k* – reaction rate constant, *k'* – substitute reaction rate constant - C_{O2} – concentration O_2, *n* – reaction order versus O_2 concentration O_2.

After separating the variables and integrating the equation can be presented in the form (2):

$$\int \frac{dX}{f(X)} = k' \int dt \quad (2)$$

And after transformation:

$$g(X) = k' \cdot t \quad (3)$$

where: *g(X)* – chemical reaction model for the integral form of the kinetic equation, *t* – reaction time to achieve the degree of the conversion X.

Reaction model

The models of analyzed reactions were summarized in Tab.3. In general, models can be divided into the following groups: F, R, D, A. Models included in group F represent the reaction rate as reactions in a homogeneous phase of a specific order. The R group represents geometric models, where the reaction takes place on the surface of a particular geometric form, i.e. a flat surface, an infinitely long cylinder and a sphere. Similarly, models D represent identical geometries but they take into account the presence of an outer layer which results in diffusion resistance and that is the limiting factor for the reaction rate.

Group A model has been developed for the crystallization, where there is the occurrence of nuclei (induction period) and then their growth. A detailed discussion of the models can be found in Brown work [24]. A separate model is the random pore model, which, unlike the rest of the models, is applied to the structure of a porous substance. Due to the multiplicity of existing models, there is usually a problem of choosing the right one.

Table 3 Kinetic models applied in calculations [24]

Model	$f(X)$	$g(X)$
F0	*1*	X
F1	$1-X$	$-ln(1-X)$
R2	$2(1-X)^{1/2}$	$1-(1-X)^{1/2}$
R3	$3(1-X)^{2/3}$	$1-(1-X)^{1/3}$

RPM	$(1-X)\sqrt{1-\psi ln(1-X)}$	$\frac{2}{\psi}\left(\sqrt{1-\psi ln(1-X)}-1\right)$
D2	$(-ln(1-X))^{-1}$	$(1-X)l\,n(1-X)+X$
D3	$\frac{3}{2}(1-X)^{2/3}\left(1-(1-X)^{1/3}\right)^{-1}$	$\left(1-(1-X)^{1/3}\right)^{2}$
A2	$2(1-X)(-l\,n(1-X))^{1/2}$	$(-l\,n(1-X))^{1/2}$

The modelling of kinetic data was conducted for both data approaches i.e. integral, and differential, to determine the impact of these data, as well as the computational methodology on the results of the calculated reaction rate constant. For this reason, in house developed own computing codes in the MathCad Prime 2.0 software was applied. Furthermore, for the purpose of this analysis the reaction rate constant k' was calculated from two equations (1) - $k'_{f(X)}$ – differential form, and from integral form (3) - $k'_{g(X)}$

For conformity assessment of the model with experimental data, an additional statistical function as a sum of the squared error (SSE) can be applicated. The residual components are the differences between the model value and the experimental value and they determine the inaccuracy of the model determination. The sum of their squares divided by the number of measurement points and reduced by the number of estimated parameters of the regression function (for the linear function k = 2) is the average square error (variance of the residual component) and is expressed by the relationship [25] (4):

$$S^2=\frac{1}{n-2}\sum_{i=1}^{n}\left(\left(\frac{dX}{dt}\right)_i-k'\cdot f(X)_i\right)^2 \tag{4}$$

The analysis was carried out for data obtained for each temperature and for each model. The procedure consists in finding the minimum value S^2 appropriate for a given model and selecting the best fitted model using the F-fitting index calculated from the equation (5)

$$F=\frac{S^2}{S^2_{min}} \tag{5}$$

The index shows the ratio of the sum of square errors of the model for a given temperature to the lowest sum of square errors for the best fitted model. The F factor indicates therefore the number of times the average square error of a given model is greater than the lowest square error for the best fit model.

A similar factor has been used for the data of the integral model and is presented by the dependence (6):

$$\mathrm{S^2}=\frac{1}{\mathrm{n}-2}\sum_{\mathrm{i}=1}^{\mathrm{n}}(\mathrm{g(X)_i}-\mathrm{k'}\cdot\mathrm{t_i})^2 \tag{6}$$

and the fitting factor will also be represented by the relationship (5).

The models presenting the rate of the chemical reaction, diffusion and penetration of O_2 to the surface of the char beds in the TG's crucible were widely discussed in the publication of authors [26]. These models are expressed by the following relationships (7):

$$r_{eff}=\left(\frac{1}{r_R}+\frac{1}{r_D}\right)^{-1} \tag{7}$$

Where (8):

$$r_R = f(X)C_{O2}^n k_R = f(X)C_{O2}^n A_0 \exp\left(\frac{-E_a}{\mathrm{R}\cdot T}\right) \quad (8)$$

The O_2 transport rate to the chars bed in the TG's is expressed by the equation (9):

$$r_D = \frac{Sh \cdot D_{O2}}{d_N} A_N \frac{C_{O2,2}}{2} \quad (9)$$

where: D_{O2} – bulk O_2 diffusion coefficient, A_N surface of the chars particles in a bed.

Influence of pressure and oxygen concentration

Main factors influencing the rate of oxycombustion reaction are: oxygen concentration, oxygen partial pressure, total pressure and oxygen molar fraction. Total pressure and oxygen partial pressure are independent parameters. There is a functional relation between these two parameters i.e..: the ratio of the oxygen partial pressure to the total pressure is the oxygen molar fraction and is expressed by the relation (10):

$$y_{O2} = \frac{P_{O2}}{P_t} \quad (10)$$

where: y_{O2} – oxygen molar fraction in gas, P_t – total gas pressure, P_{O2} – oxygen partial pressure.
Oxygen concentration as number of moles of O_2 particles in unit volume is a function of oxygen partial pressure and temperature, and can be expressed by the relation (11):

$$C_{O2} = \frac{P_{O2}}{R \cdot T}, \frac{mol}{m^3} \quad (11)$$

where: C_{O2} – oxygen molar concentration for given partial pressure and temperature, P_{O2} – oxygen partial pressure.

The overall reaction rate is the assembly of two modules, i.e.: chemical reaction rate and oxygen transport rate. Different factors have key impact on each of these modules. The rate of the chemical reaction is essentially influenced by the oxygen partial pressure (indirectly by oxygen concentration), and for the oxygen transport rate key factor is the ratio of the oxygen partial pressure to the total pressure, i.e., the molar fraction.

It can be then stated that reaction rate of oxycombustion is independent from total pressure. In these cases kinetic equation can be rewritten as (12):

$$r_{og} = r_R = k_R \cdot f(X) \cdot C_{O2}^n \quad (12)$$

Logarithm of equation (12) gives relation allowing to calculate reaction order in function of oxygen concentration (13)

$$ln(r_R) = n \cdot ln(C_{O2}) + ln(k_R \cdot f(X)) \quad (13)$$

Results and Discussion

Selection of reaction model

The results of TGA experiments and kinetic analysis are presented both as the integral form, i.e. graphs of the degree of conversion as a function of time, and in the differential form as the reaction rate as a function of extent of conversion. That's the reason why the rate constant k' can be calculated from both equations (1) and

(3). The integral method consists of determining the function of integrating the model response within the prescribed period of time. The differential method consists in approximating the derivative of the degree of conversion in time by means of finite differences (increments), and the finite differences should be chosen in such a way that they are as small as possible. Differences between these methods result from the accuracy of the approximation of the function describing the reaction model to the experimental data. Apparently, the accuracy of the integral method is greater than the differential one, because it is the sum of infinitely many elements. However, this causes fitting of model to the whole range from 0 to X, which may result in reducing the differences between models. In the case of the differential method, the fitting takes place on the given infinitesimal stretch of dX regardless of the previous course. For this reason, the differential method, despite its formal lower accuracy, may clearly differentiate the fit of the models to the experimental data.

Fig.1 and Fig.2 show the models' fitting to experimental values for integral (a) and differential data (b) for Turów and Janina chars, respectively, obtained from experiments carried out at a pressure of 0.1 MPa and using a gas containing 20% O_2 / CO_2.

a)

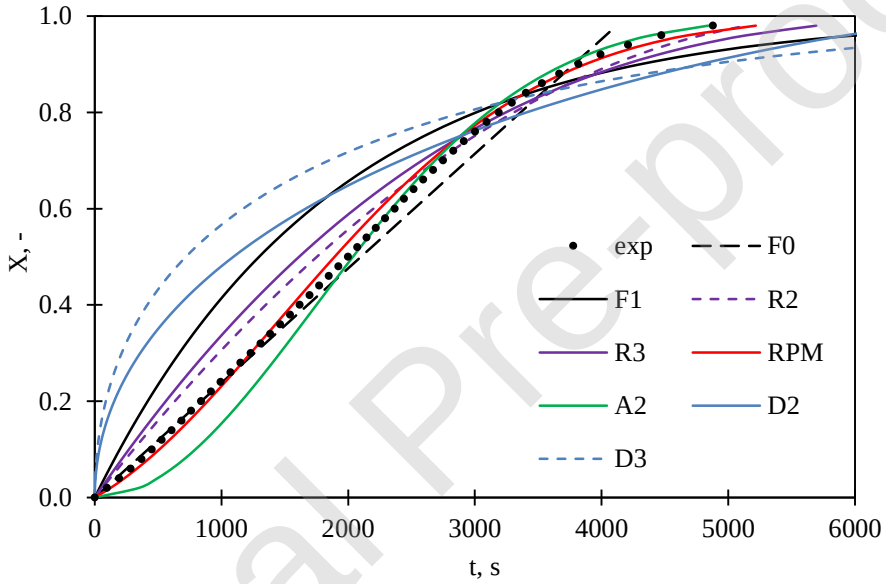

b)

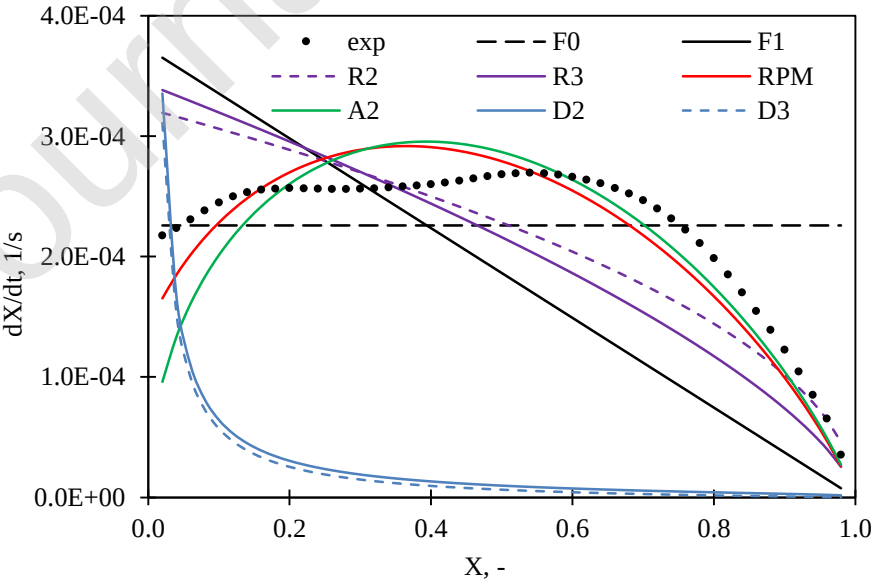

Fig. 1 Fitting of various models for Turow char oxycombustion in a mixture of 20% O_2 / 80% CO_2 at 0.1MPa for integral (a) and differential data (b). Reaction was carried out in HPTGA.

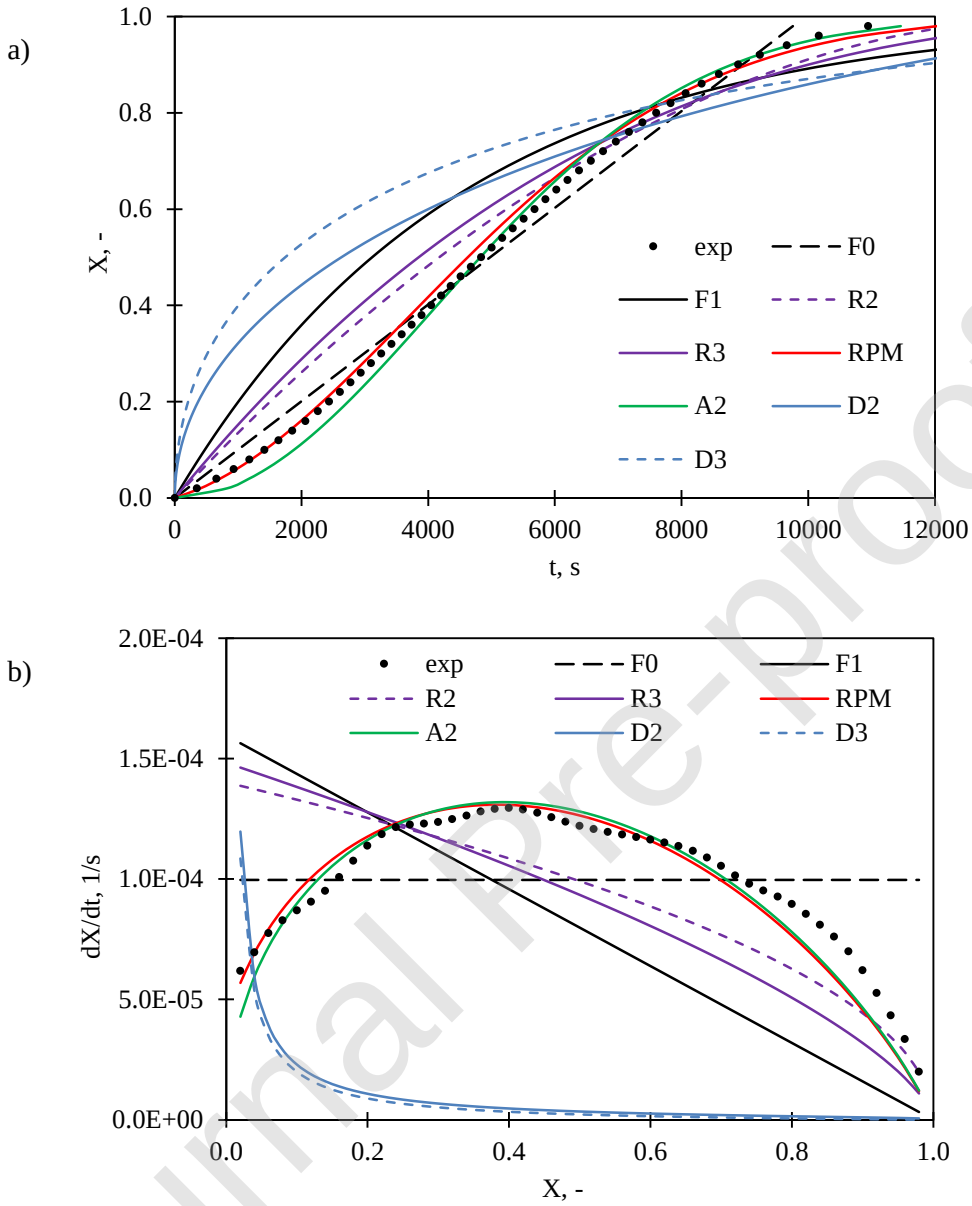

Fig. 2 Fitting of various models for Janina char oxycombustion in a mixture of 20% O_2 / 80% CO_2 at 0.1MPa for integral (a) and differential data (b). Reaction was carried out in HPTGA.

The models presented on the charts can be divided into three groups being a function: constant because of the degree of conversion of X - F0 model;- constantly decreasing: R2 and R3 models; highly decreasing in the first stage: D2 and D3; in the first stage increasing, and after reaching the maximum decreasing (RPM and A2). The D2 and D3 model are much different than other models and will be not further taken into account.

The above figures clearly indicate that the best fit is RPM model is and it explains the course of the oxycombustion reaction in best way, however the A2 model also seems to have a good fit. This is particularly evident for differential data that represents the course of reaction rate as a function of the degree of conversion of X. This statement on the basis of integral data (the degree of conversion as a function of reaction time) would

raise doubts due to the relatively small differences between experimental and model values. This is the main reason for choosing a differential method to select an appropriate reaction model.

The above figures show one more important aspect of the fit of the model to the reaction data, namely the mathematical differences between the models. The models of RPM and A2 in their mathematical form are very similar, although they are based on completely different theoretical foundations [24,27,28]. The average relative square error between the two models for the differential form can be represented by a relationship (14):

$$S^2 = \frac{1}{n-2}\sum_{i=1}^{n}\left(\frac{k'_{RPM}\cdot f_{RPM}(X)_i - k'_{A2}\cdot f_{A2}(X)_i}{k'_{RPM}\cdot f_{RPM}(X)_i}\right)^2 \quad (14)$$

and for the integral form relative square error can be represented by a relationship (15):

$$S^2 = \frac{1}{n-2}\sum_{i=1}^{n}\left(\frac{\frac{k'_{RPM}}{g_{RPM}(X)_i} - \frac{k'_{A2}}{g_{A2}(X)_i}}{\frac{k'_{RPM}}{g_{RPM}(X)_i}}\right)^2 \quad (15)$$

The calculated error for oxycombustion of Turów char for the differential form is 0.86% and for Janina char is equal to 0.23%, which is a slight difference in both cases. In this case, the integral form differentiates both models more clearly and the relative errors between the models are 14.96% and 5.04% respectively for the Turów and Janina chars. The calculated relative error between the models RPM and A2 indicates that in the case of model analysis, the distinction of these models is better for the integral method than for the differential method. This is the opposite situation than in the case of other models, where the differences between the models are greater for the differential form than for the integral method, e.g.: the relative error between R2 and RPM is 8.08% and 12.46% for the differential form for Turów and Janina, respectively, and for the integral form 4.47% and 6.81% for Turów and Janina, respectively.

The differential method clearly delimits different reaction models between each other, which makes the selection of the model based on the visual selection easier, except the case of the RPM and A2 models discussed above. Therefore, the model selection should be done using differential and integral data. The key issue is also the comparison and ranking of the models based on the variance of the residual component (mean square error) calculated from the equation (14), the results of which are presented in Tab. 4 and Table 5. The presented ranking shows how many times the average square error of a given model is greater than the average square error of the best fit model (with the lowest mean square error). The tables also show the sums and medians of individual adjustment ratios for all applicable temperatures, which helps with a comprehensive assessment taking into account the results obtained from different temperatures. Using the presented methodology, the ranking of models was made for successive matrixes of experiments, i.e. oxycombustion of Turów char (Tab. 4) and Janina char (Tab. 5) for 20 and 30% O_2 concentration in CO_2 and for 0.1, 0.5 and 1.0 MPa.

Table 4 Ranking of models' fitting for Turów oxycombustion.

P_t, MPa	O_2 concentration		**F0**	**F1**	**R2**	**R3**	**RPM**	**A2**
0,1 MPa	20% O_2	$F_{f(X)}$	5,2	7,5	2,5	4,1	1,0	2,5
		$F_{g(X)}$	8,0	413,4	3,2	3,9	1,0	32,0
	30% O_2	$F_{f(X)}$	3,0	10,1	2,3	3,7	1,0	1,8
		$F_{g(X)}$	3,6	343,9	4,0	5,2	1,0	12,4

0,5 MPa	20% O_2	$F_{f(X)}$	1,5	9,3	3,1	4,8	1,0	1,9
		$F_{g(X)}$	1,5	250,5	2,9	3,4	1,0	7,5
	30% O_2	$F_{f(X)}$	3,4	4,2	1,4	2,2	1,1	1,0
		$F_{g(X)}$	7,6	377,9	8,9	8,4	1,0	15,9
1,0 MPa	20% O_2	$F_{f(X)}$	6,5	20,0	7,4	11,3	1,0	1,1
		$F_{g(X)}$	7,8	761,3	12,2	15,4	1,0	10,5
	30% O_2	$F_{f(X)}$	4,0	15,1	6,6	9,4	1,0	1,7
		$F_{g(X)}$	1,8	117,9	2,8	2,9	1,0	3,9

Table 5 Ranking of models' fitting for Janina oxycombustion.

P_t, MPa	O_2 concentration		**F0**	**F1**	**R2**	**R3**	**RPM**	**A2**
0,1 MPa	20% O_2	$F_{f(X)}$	10,7	30,0	5,0	14,3	1,0	1,8
		$F_{g(X)}$	36,5	1677,8	13,7	19,1	1,0	29,9
	30% O_2	$F_{f(X)}$	4,2	10,0	1,1	3,2	1,0	2,1
		$F_{g(X)}$	6,7	692,6	7,2	10,2	1,0	34,5
0,5 MPa	20% O_2	$F_{f(X)}$	4,1	6,3	1,4	2,7	1,0	1,5
		$F_{g(X)}$	15,9	737,0	8,6	8,6	1,0	31,3
	30% O_2	$F_{f(X)}$	2,7	5,4	1,1	2,3	1,0	1,4
		$F_{g(X)}$	13,6	639,0	6,3	9,2	1,0	51,7
1,0 MPa	20% O_2	$F_{f(X)}$	4,0	13,0	5,1	7,6	1,4	1,0
		$F_{g(X)}$	14,8	672,5	7,8	8,4	1,0	31,2
	30% O_2	$F_{f(X)}$	3,4	9,9	3,3	5,0	1,1	1,0
		$F_{g(X)}$	7,8	761,3	12,2	15,4	1,0	10,5

Based on the rankings made, it can be unequivocally stated that the RPM model shows the best fit in the entire matrix of experiments. In some cases, the A2 model, which was developed for the crystallization process, turns out to be better. The A2 model therefore describes the nucleation reaction, where in the initial stage there is an induction period, i.e. the generation of nucleation seeds. The RPM model, on the other hand, describes the course of reaction on the surface of the pores and presents essentially changes in the internal surface during the reaction. The relative error between the models RPM and A2 is 0.86% and 0.23% for the Turów and Janina chars respectively, so there are cases where the A2 model also shows a good fit.

Mathematical selection based on the analysis of the mean square error and model ranking clearly indicates the RPM model as the best fit model. Therefore, the adjustment of individual models for differential data for char oxycombustion for thermogravimetimeter HPTGA and Netzsch STA 409 PG Luxx it is presented in Fig. 3 - Fig. 6.

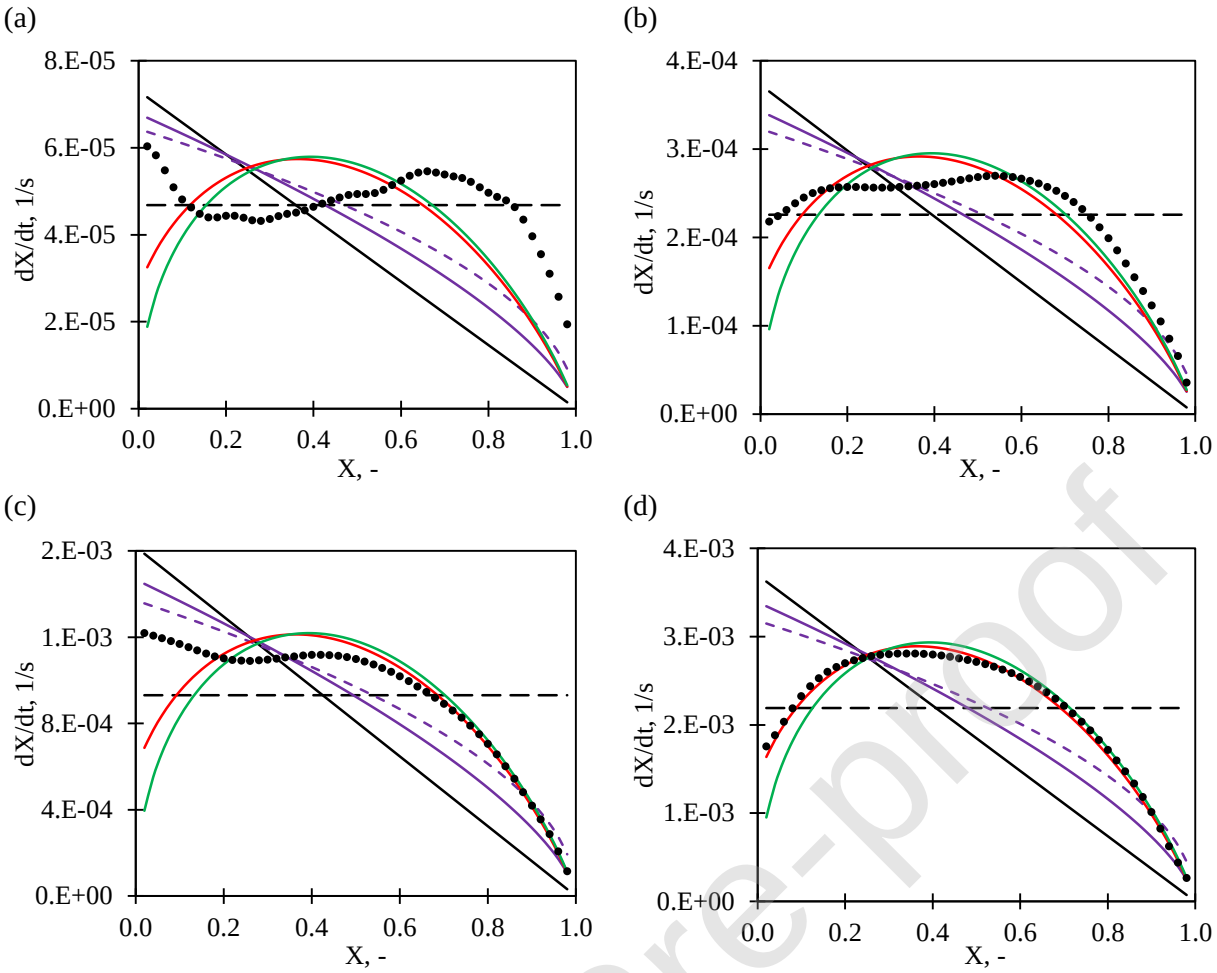

Fig. 3 Reaction rate of the char oxycombustion of Turów and fitting the models: — — model F0, — — model F1, – – – model R2, —— model R3, —— model RPM, —— model A2, ● the experimental value of the reaction rate, for subsequent reaction temperatures: (a) - 450°C, (b) - 500°C, (c) - 550°C, (d) - 600°C (20% O_2 in CO_2 total pressure 0,1MPa)

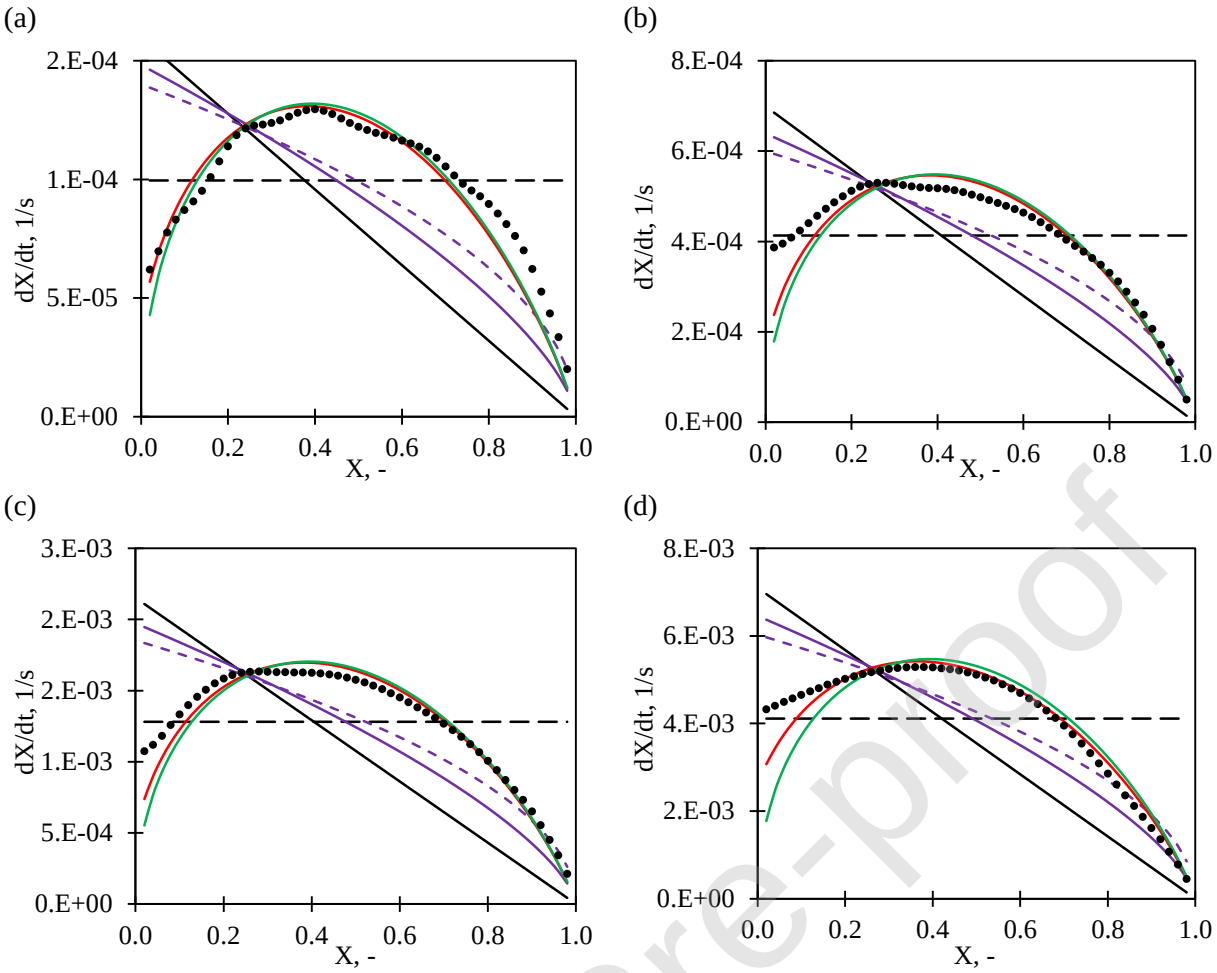

Fig. 4 Reaction rate of the char oxycombustion of Janina and fitting the models:: — — model F0, — — model F1, – – – model R2, —— model R3, —— model RPM, —— model A2, ● the experimental value of the reaction rate, for subsequent reaction temperatures:: (a) - 500°C, (b) - 550°C, (c) - 600°C, (d) - 700°C (20% O_2 in CO_2, total pressure 0,1MPa)

The figures presented above clearly indicate that the model with the best fit is the random pore model, however, the RPM model as a function of the conversion rate also shows less regular courses. Fit of the RPM model to the results of the Janina char oxycombustion process shows a good correlation between the experimental results and the results of the model analysis. However, in the case of Turów char oxycombustion reaction, there are deviations of experimental results from the RPM model, especially in the initial reaction stage. In the initial stage, the reaction rate decreases or remains unchanged up to the conversion rate of approx. 0.2. Then, the reaction rate stabilizes at a similar level or slightly increases, so that above the conversion rate X = approx. 0.6-0.7 decrease to a value of 0.

The above changes in the reaction rate or the constant rate of oxidation reaction result from the fact that the parameter ψ in the RPM model is assumed as a constant value, which refers to the initial properties of the porous chars structure.

This model closely defines the structural parameter of fuel ψ, the value of which depends not only on the measurable specific surface, but also on the structure and number of pores (16):

$$\psi = \frac{4\pi L_0(1-\varepsilon_0)}{S_{V,0}^2}$$

where: L_0 - initial pore length in the system related to the volume unit, ε_0 - initial porosity of the char.

The structural parameter ψ can be calculated on the basis of the above dependence based on measurements of the "initial" characteristic properties or it can be determined experimentally. However, during the reaction occur changes in the structure of the porous chars, which indirectly influents on the observed reaction rates as a function of the C element conversion. In particular, in the initial stage, may occur the largest and most significant changes in the structure and therefore irregularities may be observed in the course of the reaction rate in the initial reaction stage.

The reason for differences between the rates of reaction rate as a function of the degree of conversion for oxycombustion process of both chars may be due to differences between these chars. Both chars have different properties of the porous structure, with the structure of the Turów char being more developed, properties presented in Table 1 and in Table 2 i.e. characterization of the structure of carbonates obtained by sorption of N_2 and CO_2 vapours, characterization of the structure of chars obtained by mercury porosimetry.

Influence of oxygen concentration on reaction rate of oxycombustion

Influence of oxygen concentration on reaction rate of oxycombustion under total pressures 0.1 and 1.0 MPa for both chars at 500°C (kinetic regime of reaction) is shown on Fig. 5 and 6.

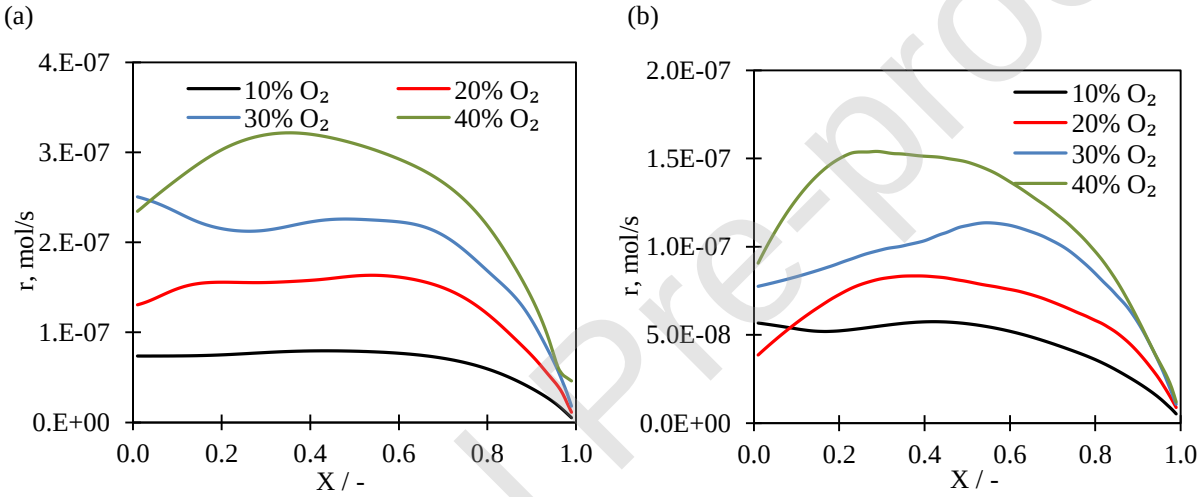

Fig. 5. Influence of oxygen concentration on reaction rate of oxycombustion under total pressure 0.1MPa for chars Turów (a) and Janina (b) in HPTGA

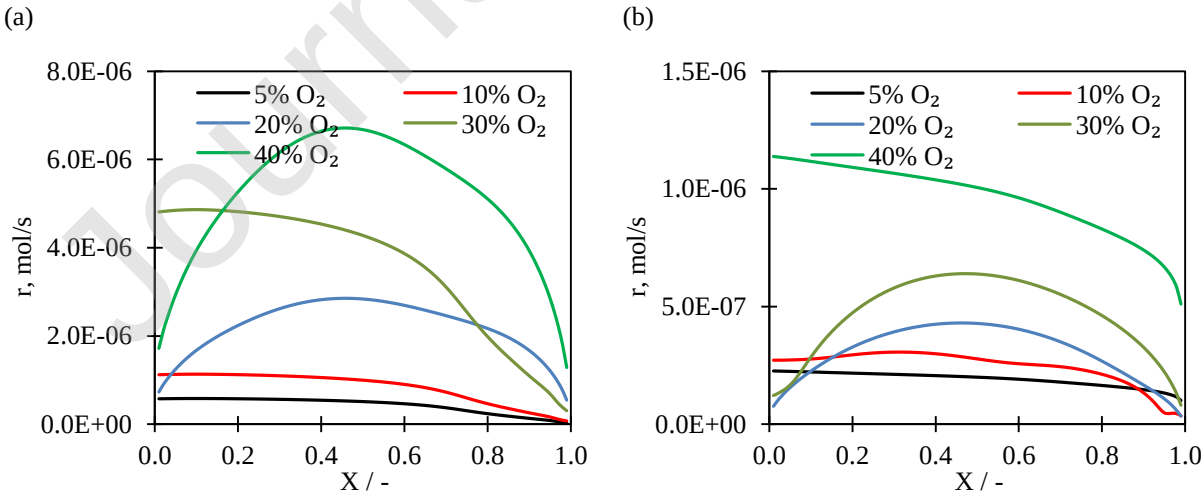

Fig. 6. Influence of oxygen concentration on reaction rate of oxycombustion under total pressure 1.0 MPa for chars Turów (a) and Janina (b) in HPTGA

It can be noticed in above figures that increase of oxygen concentration in O_2/CO_2 mixture causes growth of reaction rate of oxycombustion under constant total pressure. Positive influence of oxygen partial pressure or oxygen concentration under atmospheric pressure are fully consistent with the literature [29- 31]. Influence of oxygen concentration on reaction rate of oxycombustion was also studied under higher total pressures. Reaction rates in function of oxygen molar volumetric concentration expressed as a number of O_2 moles per volume unit mol/m^3 are shown on Fig. 7 for all total pressures and concentrations.

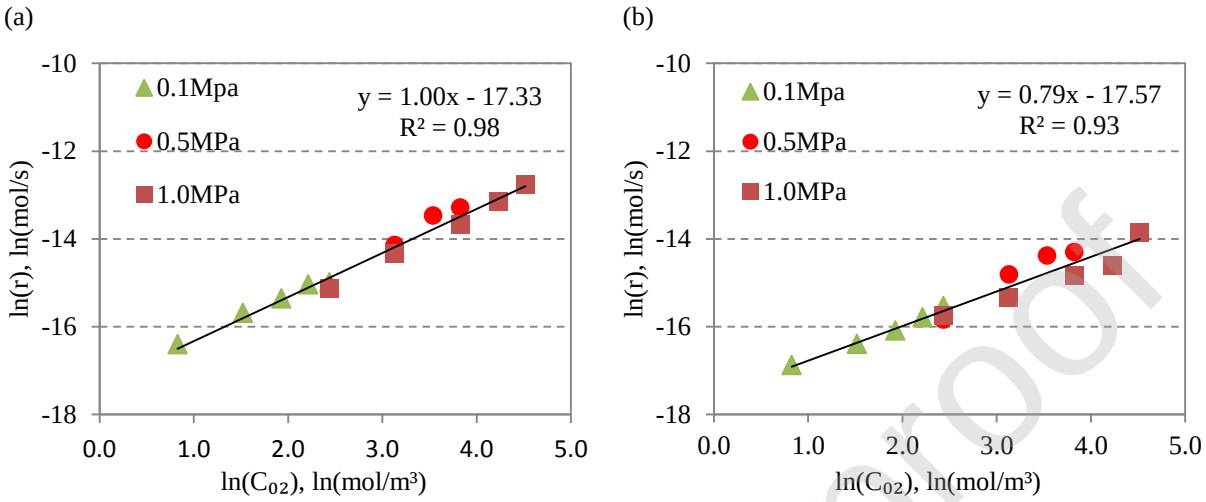

Fig. 7. Influence of oxygen concentration (O_2 partial pressure) on reaction rate of oxycombustion for chars Turów (a) and Janina (b) in HPTGA

Analysis of above date leads to conclusion that for both chars a linear increase of reaction rate with increasing oxygen concentration is observed under all used pressures. Experiments were conducted at 500°C so in kinetic regime of reaction where influence of mass transfer is negligible. It can be then stated that reaction rate of oxycombustion is independent from total pressure.

Basing on data of reaction rate in function of oxygen concentration an estimation of reaction order with oxygen concentration was performed. Calculated reaction order for Turów char equals 1.00 with high correlation coefficient of 0.97. Identical correlation for Janina char gives reaction order equal 0.79 with significantly lower correlation coefficient of 0.93.

Differences observed in values of reaction order for both chars are mainly due to share of available active sites in oxycombustion reaction [30, 32]. Rate of reaction is namely dependent on contribution of char active substance which is C element and decreases with the decreasing share of this substance and the possibility of creating active sites. Changes of rate of reaction can be correlated with parameter expressing ratio of C element share to mineral substance in char. Calculated value of that parameter equals 5.58 and 7.11 for Janina and Turów chars respectively. Ratio of these values is equal 0.81 when ratio of reaction orders is equal 0.79. It confirms a dependence between reaction rate of oxycombustion and active substance share which is C element in char.

Above analysis indicates that in kinetic regime reaction rate of oxycombustion is proportional to oxygen concentration in feed gas. Rate of reaction is characteristic for each char and should be determined separately.

Influence of total pressure

In order to analyze the influence of total pressure on oxycombustion reaction rate experiments under three different total pressures were conducted with the same oxygen partial pressure equal 0.05 MPa, and oxygen concentration of 11.3 mol/m^3. Comparison of reaction rates for above conditions are shown on figure 8.

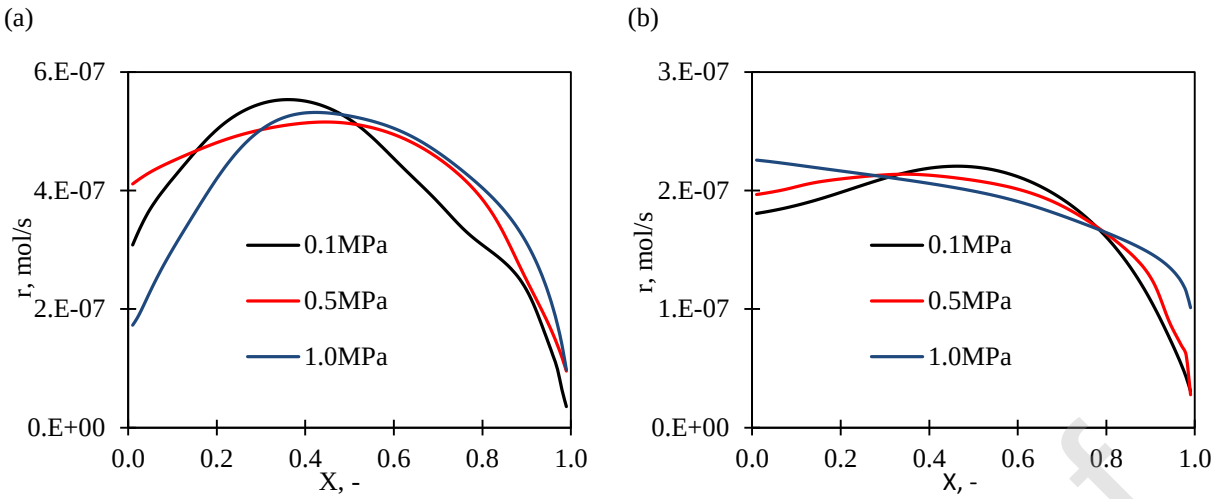

Fig. 8. Influence of total pressure at constant oxygen partial pressure (0.05 MPa, 11.3 mol/m^3 O_2) on oxycombustion reaction rate of chars Turów (a) and Janina (b) in HPTGA

Analyzing data on above figure leads to conclusion that in kinetic regime there is no influence of total pressure at constant oxygen partial pressure on reaction rate of oxycombustion. It is a confirmation of the assumed chemical reaction model that takes into account only the influence of oxygen concentration on the chemical reaction rate and does not take into account the influence of total pressure.

Global impact of oxygen concentration and total pressure

Reaction rate of oxycombustion is the result of the resistance of both the chemical reaction and diffusion processes as shown in equation (8). In this study model from publication of authors was applied [26] which can be expressed by (Eq. 17):

$$r_D = \dot{N}_{O2} = \frac{D_{O2,0}}{l_D} T^{0,75} A_N \left(y_{O2,1} - y_{O2,2}\right), \frac{mol}{s} \quad (17)$$

where: $D_{O2,0}$ – molecular diffusion coefficient at T = 273 K and P_t = 1.013·10^5 Pa

The rate of oxygen transport processes is therefore not dependent on total pressure but on oxygen partial pressure in feed gas. In diffusion regime only influence of molar fraction on oxycombustion reaction rate is observed and with increasing oxygen molar fraction rate of O_2 transport increases.

Kinetic parameters of isolated chemical reaction were calculated and shown in Tab. 6. Activation energy is determined from experiments with feed gas containing 20% O_2 in CO_2 under pressure 0.1 MPa and is consistent for whole range of total pressure. Reaction order were determined at 500°C.

Table 6. Kinetic parameters of oxycombustion of chars in pressure range from 0.1 to 1.0 MPa

	Turów char	**Janina char**
Activation energy, E_a, kJ/mol	147,3	142,4
Preexponential factor, $ln(A_0)$, ln((m^3) $^{1/n}$ /s)	6,88	4,77
Reaction order vs O_2, n, -	1,00	0,79
Ψ parameter in RPM model	21	58

Inserting above data to elaborated chemical reaction model we obtain results of model analysis for whole range of temperature and total pressure. Results were correlated with experimental values of chars oxycombustion obtained under whole range of total pressure i.e. 0.1, 0.5 and 1.0 MPa and oxygen concentration 20 and 30% in CO_2. Results of correlation are shown on figures 9 and 10.

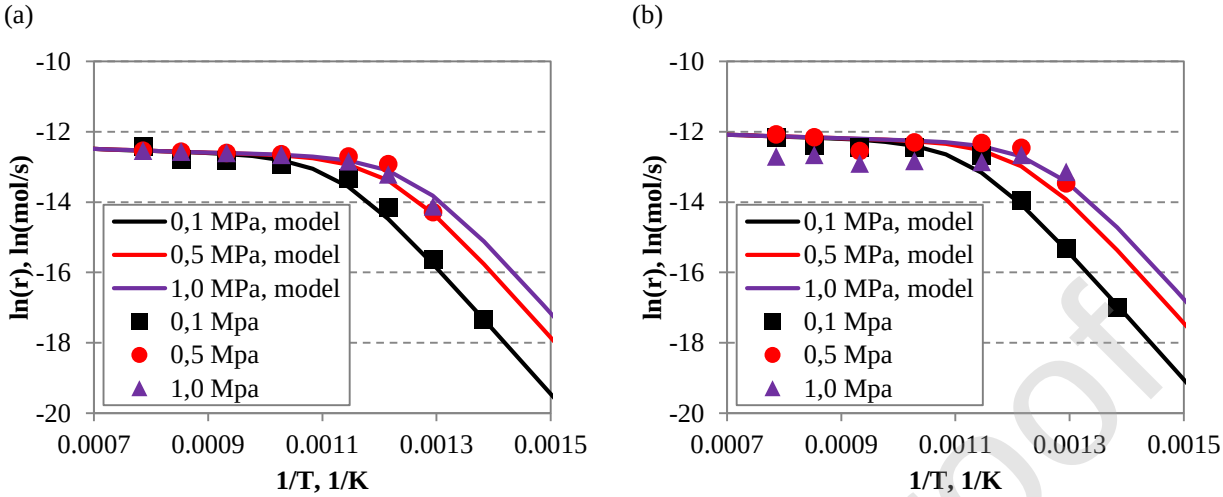

Fig. 9. Reaction rate in function of temperature reciprocal for oxycombustion of Turów char in gas containing 20% O_2 (a) and 30% O_2 (b) in HPTGA

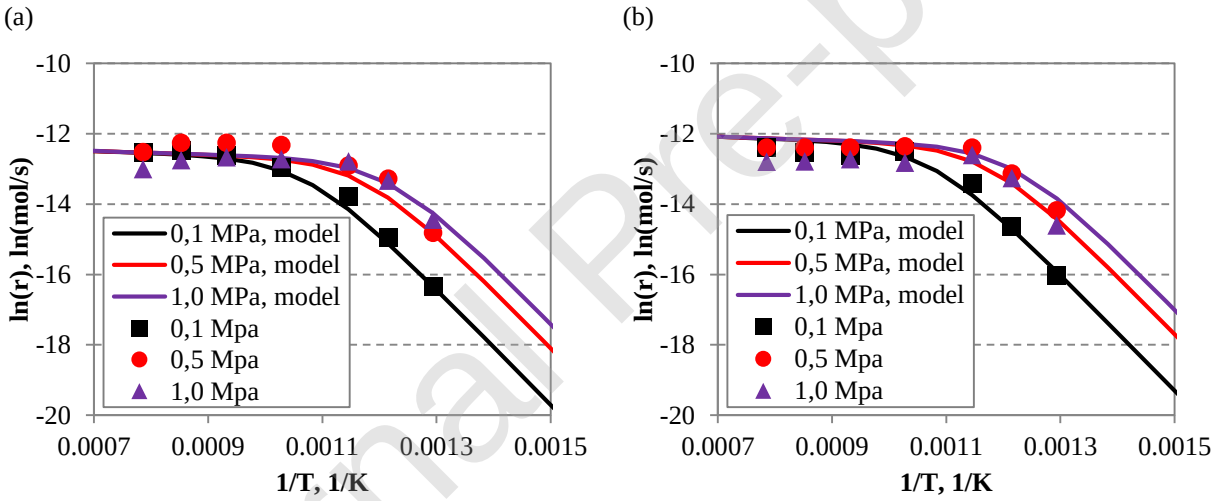

Fig. 10. Reaction rate in function of temperature reciprocal for oxycombustion of Janina char in gas containing 20% O_2 (a) and 30% O_2 (b) in HPTGA

Results of above analysis indicates that with increasing total pressure reaction rate in kinetic regime increases. This is due to the fact that increase of total pressure at constant oxygen molar fraction in feed gas (for example 20% O_2 in CO_2) increases O_2 partial pressure and this is essential reason of reaction rate growth.

In diffusion regime oxygen transfer rate does not depend on total pressure but O_2 molar fraction in feed gas. For that reason reaction rates in diffusion regime are close to each other and relatively independent of total pressure. Small differences in reaction rates can be noticed on figures in diffusion regime, in particular between reaction rates under 0.5 and 1.0 MPa. The reason for these differences is total pressure, however acting in this case in completely different way.

Conclusions

- Use of increased pressure influence positively the kinetics of coal oxycombustion reaction due to increase of O_2 molar volumetric concentration. Increase of total pressure causes only apparently increase of reaction rate which is in fact secondary to increase of O_2 concentration in feed gas.
- Reaction rate of oxycombustion in kinetic regime is proportional to oxygen concentration raised to the power of reaction order.
- Kinetic parameters of oxycombustion reaction are constant for pressure range from 0.1 to 1.0 MPa and describes reaction rate in function of oxygen concentration.
- Selection of the appropriate reaction model must be based on the correlation of differential data not integral data (conversion rate as a function of reaction time). Differences between these methods result from the accuracy of the approximation of the function describing the reaction model to the experimental data.
- Random pore model (RPM) is an appropriate model describing the rate of oxycombustion reaction of coal char.

Acknowledgement:

This scientific work was supported by the National Centre for Research and Development, as Strategic Project PS/E/2/66420/10 "Advanced Technologies for Energy Generation: Oxy-combustion technology for PC and FBC boilers with CO_2 capture". The support is gratefully acknowledged.

This work was partially financed from the People Programme (Marie Curie Actions) of the European Union's Seventh Framework Programme FP7/2007–2013/ under REA grant agreement n° PIRSES–GA–2013–612699 entitled "Long–term research activities in the area of advanced CO_2 capture technologies for Clean Coal Energy Generation – "CO2TRIP and by the Polish Ministry of Higher Education and Science, Decision No. 3111/7.PR/2014/2 as "Scientific work financed from the funds for science in years 2014–2017, allocated for completion of the international co–financed project", and also from subsidy project.

Literature

[1] L. Stroemberg, Combustion in a CO_2/O_2 mixture for a CO_2 emission free process, 2nd Nordic Minisymposium on Carbon Dioxide Capture and Storage, 26.10.2001, Göteborg

[2] B. J. P. Buhre, L. K. Elliot, C. D. Sheng, R. P. Gupta, T.F. Wall, Oxy-fuel combustion technology for coal-fired power generation, Prog. Energy Combust. Sci. 31 (2005) 283–307. doi:10.1016/j.pecs.2005.07.001

[3] J. Lasek, K. Głód, M. Janusz, K. Kazalski, J. Zuwała, Pressurized oxy-fuel combustion: A Study of selected parameters, Energy Fuels 26 (2012) 6492–6499. doi:10.1021/ef201677f

[4] J. Lasek, M. Janusz, J. Zuwała, K. Głód, A. Iluk, Oxy-fuel combustion of selected solid fuels under atmospheric and elevated pressures. Energy, 62 (2013) 105–112. doi:10.1016/j.energy.2013.04.079

[5] J. Dubiński, A. Koteras, Przyszłość węgla jako paliw energetycznego, Przegląd Górniczy, 2012, 68, 12, 8–12 (In Polish)

[6] J. Hong, G. Chaudhry, J.G. Brisson, R. Field, M. Gazzino, A. F. Ghoniem, Analysis of oxy-fuel combustion power cycle utilizing a pressurized coal combustor, Energy 34 (2009) 1332–1340. doi:10.1016/j.energy.2009.05.015

[7] J. Hong, R. Field, M. Gazzino, A.F. Ghoniem, Operating pressure dependence of the pressurized oxy-fuel combustion power cycle, Energy 35 (2010) 5391–5399. doi:10.1016/j.energy.2010.07.016

[8] T. F. Wall, Y. Liu, Ch. Spero, L. K. Elliott, S. Khare, R. K. Rathnam, F. Zeenathal, M. Behdad, B. Buhre, Ch. Sheng, R. Gupta, T. Yamada, K. Makino, J. Yu, An overview on oxyfuel coal combustion: State of the art research and technology development, Chemical Engineering Research and Design 87 (2009) 1003–1016. doi:10.1016/j.cherd.2009.02.005

[9] L. Ma, R. Mitchell, Modeling char oxidation behavior under Zone II burning conditions at elevated pressures, Combust. Flame. 156 (2009) 37–50. doi:10.1016/j.combustflame. (accessed 2008.06.015)

[10] D.G. Roberts, Intrinsic reaction kinetics of coal chars with oxygen, carbon dioxide and steam at elevated pressures, Ph.D. Thesis, University of Newcastle 2000.

[11] W. Kordylewski, Fuel Combustion, Publishing House: Oficyna Wydawnicza Politechniki Wrocławskiej, Wrocław 2008. In Polish.

[12] T.F. Wall, Y. Liu, Ch. Spero, L. Elliott, S. Khare, R. Rathnam, F. Zeenathal, B. Moghtaderi, B. Buhre, Ch. Sheng, R. Gupta, T. Yamada, K. Makino, J. Yu, An overview on oxyfuel coal combustion: State of the art research and technology development. Chem. Eng. Res. Des. 87 (2009) 1003–1016. doi:10.1016/j.cherd.2009.02.005

[13] I.W. Smith, The combustion rates of coal chars: a review. 19th Symposium on Combustion, Proc. Combust. Inst. 19 (1982) 1045–1065.

[14] T. Czakiert, Z. Bis, W. Muskala, W. Nowak, Fuel conversion from oxy-fuel combustion in a circulating fluidized bed, Fuel Process. Technol. 87 (2006) 531–538. doi:10.1016/j.fuproc.2005.12.003

[15] A. Gomez-Barea, P. Ollero, R. Arjona, Reaction-diffusion model of TGA gasification experiments for estimating diffusional effects, Fuel 84 (2005) 1695–1704. doi:10.1016/j.fuel.2005.02.003

[16] S. Salvador, J.M. Commandre, B.R. Stanmore, Reaction rates for the oxidation of highly sulphurised petroleum cokes: the influence of thermogravimetric conditions and some coke properties, Fuel 82 (2003) 715–720. doi:10.1016/S0016-2361(02)00363-0

[17] P. Babiński, G. Łabojko, A. Plis, M. Kotyczka – Morańska, Kinetics of coal and char oxy-combustion studied by TG-FTIR, J Therm Anal Calorim. 113 (2013) 371–378. doi:10.1007/s10973-013-3002-x

[18] P. Babiński, M. Tomaszewicz, T. Topolnicka, M. Ściążko, J. Zuwała, Tlenowe spalanie węgla: badania kinetyki i mechanizmu spalania ciśnieniowego, Przemysł Chemiczny 94 (2015) 450-456, In Polish. doi:10.15199/62.2015.4.2

[19] E. Ksepko, M. Ściążko, P. Babinski, Studies on the redox reaction kinetics of Fe_2O_3–CuO/Al_2O_3 and Fe_2O_3/TiO_2 oxygen carriers, Applied Energy 115 (2014) 374–383. doi:10.1016/j.apenergy.2013.10.064

[20] E. Ksepko, P. Babinski, A. Evdou, L. Nalbandian, Studies on the redox reaction kinetics of selected, naturally occurring oxygen carrier, J Therm Anal Calorim. 124 (2015) 137–150. doi:10.1007/s10973-015-5107-x

[21] S. Vyazovkin, A.K. Burnham, J.M. Criado, L.A. Pérez-Maqueda, C. Popescu, N. Sbirrazzuoli, ICTAC Kinetics Committee recommendations for performing kinetic computations on thermal analysis data, Thermochim. Acta. 520 (2011) 1–19. doi:10.1016/j.tca.2011.03.034

[22] S. Schulze, P. Nikrtiuk, Z. Abosteif, S. Guhl, A. Richter, B. Meyer, Heat and mass transfer within thermogravimetric analyser: From simulation to improved estimation of kinetic data for char gasification, Fuel 187 (2017) 338–348. doi:10.1016/j.fuel.2016.09.048

[23] R. Comesana, J. Porteiro, E. Granada, J.A. Vilan, M.A. Alvarez Feijoo, P. Eguia, CFD analysis of the modification of the furnace of a TG–FTIR facility to improve the correspondence between the emission and detection of gaseous species, Applied Energy 89 (2012) 262–272. doi:10.1016/j.apenergy.2011.07.029

[24] M. E. Brown, Handbook of Thermal Analysis and Calorimetry Vol. 1 Principles and Practice, Elsevier Science B.V., 1998

[25] M. Sobczyk, Statystyka, PWN, Warszawa, 2001

[26] P. Babiński, M. Ściążko, E. Ksepko, Limitation of thermogravimetry for oxycombustion analysis of coal chars, J. J Therm Anal Calorim. 133 (2018) 713–725. doi:10.1007/s10973-017-6782-6

[27] S.K. Bhatia, D. D. Perlmutter, A random pore model for fluid – solid reactions: isothermal, kinetic control, AIChE Journal, 26 (1980) 379–386. doi:10.1002/aic.690260308|

[28] J. Szekely, H. Y. Sohn, A structural model for gas—solid reactions with a moving boundary, Chemical Engineering Science, 25 (1970) 1091–1099. https://doi.org/10.1016/0009-2509(70)85053-9

[29] I.W. Smith, The combustion rates of coal chars: a review, 19th Symposium on Combustion, The Combustion Institute, 1982, 1045–1065

[30] R.H. Hurt, J.M. Calo, Semi-global intrinsic kinetics for char combustion modelling, Combustion and Flame, 125 (2001) 1138–114. https://doi.org/10.1016/S0010-2180(01)00234-6

[31] T. Czakiert, W. Nowak, Mechanizm i kinetyka spalania w modyfikowanych atmosferach gazowych, Nowe technologie spalania i oczyszczania spalin, pr. zbiorowa pod red. W. Nowaka i M. Pronobisa, Wyd. Politechniki Śląskiej, Gliwice 2010

[32] R. H. Hurt, B. S. Haynes, On the origin of power-law kinetics in carbon oxidation, Proceedings of the Combustion Institute 30 (2005) 2161–2168. doi:10.1016/j.proci.2004.08.131